Origin of Multiple Melting Endotherms in a High Hard Block Content Polyurethane. 1. Thermodynamic Investigation

A. Saiani,*,† W. A. Daunch,‡ H. Verbeke,‡ J.-W. Leenslag,‡ and J. S. Higgins†

Department of Chemical Engineering, Imperial College, Prince Consort Road, London, SW7 2BY, U.K., and Huntsman Polyurethanes, Everslaan 45-B-3078, Everberg, Belgium

Received April 5, 2001; Revised Manuscript Received September 13, 2001

ABSTRACT: The phase behavior of a set of high hard block content (50% to 100% hard segment by weight) linear thermoplastic polyurethanes has been investigated mainly via differential scanning calorimetry (DSC). The soft segment was based on a polypropylene oxide polyol end-capped with ethylene oxide and the hard segment on a 4,4′-methylene diphenyldiisocyanate (MDI) chain extended by 2-methyl-1,3-propanediol (MP-Diol). By investigating thermal behavior of the samples, it has been possible to assign the observed high-temperature endothermic transitions to the disruption of an ordered structure appearing in the hard phase under certain annealing conditions and to the microphase mixing of the soft and hard segments. These results suggest a two-step melting process: (1) melting of the ordered structure present in the hard phase; (2) microphase mixing of the soft and hard segments. Wide-angle X-ray scattering experiments gave further support to this assignment. In addition, investigation of the melt-quenched samples has shown that for a hard segment concentration lower than 65% a homogeneous mixed phase is obtained while for a hard segment concentration higher than 65% a two-phase system is obtained, one pure hard segment phase coexisting with a mixed phase with a hard/soft segment weight ratio of ∼1.8 corresponding to 65% hard segment concentration.

Introduction

Thermoplastic polyurethanes (TPU) are linear diblock copolymers typically constructed of statistically alternating soft (SS) and hard (HS) segments. Due to their numerous industrial applications these materials have received considerable attention. Many characterization techniques have been used to try to understand the relationship between chemical architecture, morphology, and mechanical properties of TPUs.[1,2] Their versatile physical properties are usually attributed to their microphase-separated structure deriving from the thermodynamic incompatibility between the soft and hard segments.

One important and intriguing feature of many commercial aromatic MDI/1,4-butanediol (BDO) based TPUs is the apparent multiple melting endotherms observed via differential scanning calorimetry (DSC). Several authors have assessed the problem of the physical or morphological origin of these transitions but still their exact origin is not fully understood.[3−7] To cast some further light on the origin of these multiple transitions, we decided to focus on a set of linear model TPUs with a relative high content of hard segments: from 50 to 100 wt %. The soft segment of our samples consist of polypropylene oxide, end-capped with ethylene oxide (PPO-EO), while the hard segment is composed of 4,4′-diphenylmethane diisocyanate (MDI), chain extended by a short diol chain: 2-methyl-1,3-propanediol (MP-Diol). The use of MP-Diol in place of the commonly used 1,4-butanediol was an attempt to lower the temperature of the melting transitions to facilitate high temperature annealing studies. For BDO-based TPUs usually the highest melting endotherm is observed around 210−230 °C[4] while in our case the highest melting endotherm was detected around 180−190 °C. Some authors have reported that at high temperature the onset of degradation can coincide with the melting transitions and therefore complicate the interpretation of the annealing studies. In this work, particular attention has been devoted to check, using thermogravimetric analysis (TGA) and gel permeation chromatography, the thermal stability of our materials in the conditions used and also to the reproducibility of the experimental results.

For 4,4′-MDI/BDO-based hard segment TPUs usually three endotherms are observed. A first so-called "annealing endotherm" is observed 20−30 °C higher than the applied annealing temperature. The two other melting endotherms are detected at higher temperatures up to 250 °C. Recently, Chen and co-workers[3] have published and extensive investigation, carried out mainly via DSC, on the origin of the so-called annealing endotherm. These authors suggested that this endotherm is related to some relaxation effects of the polymer chain in the hard segment phase due to the physical aging of the sample. In our case we were interested in the origin of the high-temperature melting endotherms and therefore we used annealing temperatures higher than the glass transition temperature of the hard segments to avoid any physical aging. Our investigation was also carried out using mainly DSC. This technique, in addition to the several endothermic transitions, allows the detection of the different glass transitions of the sample and is therefore a powerful tool to investigate the thermodynamic behavior of TPUs. In addition, in order to provide some structural evidence for the conclusions drawn from DSC, wide-angle X-ray scattering was used as complementary analytical technique.

Experimental Section

Synthesis. The polyurethane samples were synthesized via a two-step polymerization process. The soft segment used was

* Corresponding author. Permanent address: Laboratoire de Thermodynamique des Solutions et des Polymères, Université Blaise Pascal Clermont-Ferrand II/CNRS UMR 6003, 24 Avenue des Landais, 63177 Aubière, France.
† Imperial College.
‡ Huntsman Polyurethanes.

10.1021/ma0105993 CCC: $20.00
Published on Web 11/16/2001

Table 1. Average Molecular Weights and Polydispersities in Polystyrene Equivalent of the TPU Samples

sample	M_w	M_n	M_w/M_n	calcd av M_w of hard segment[a]	calcd av no. of MDI per hard segment[a]
PU-50%HS	24600	8300	3.0	3700	11
PU-65%HS	38200	12500	3.1	6900	20
PU-75%HS	43200	12500	3.5	11100	33
PU-80%HS	69800	12700	5.5	14800	44
PU-85%HS	33400	11300	3.0	21000	62
PU-90%HS	55500	13700	4.1	33300	98
PU-95%HS	57700	12700	4.5		171[b]
PU-100%HS	44200	11200	4.0		131[b]

[a] Calculated from Peeble's most probable distribution.[21,22] [b] Calculated directly from the measured molecular weight (M_w).

a commercially available polypropylene oxide based polyol, end-capped with ethylene oxide (PPO-EO), with an average molecular weight of $M_W = 3700$ ($M_n = 4400$/Daltocel F460 from Huntsman Polyurethanes). The TPUs synthesis was performed at 80 °C under a nitrogen atmosphere. At first a master batch of prepolymer based on 4,4′-methylene diphenyldiisocyanate (MDI) (Suprasec MPR from Huntsman Polyurethanes) and dried PPO-EO polyol was prepared. Then a mixture of this prepolymer and Suprasec MPR, so as to obtain the desired weight ratio between soft and hard segments, was slowly added to a preheated (85 °C) solution in dimethylacetamide (DMAC) of 2-methyl-1,3-propanediol (MP-Diol) in the presence of 0.25% catalyst (DABCO-S from Air Products), the hard segment corresponding then to the MDI and the MP-Diol (chain extender). After reaction and blending with MPR, the TPU solution was cooled to ambient temperature and was precipitated in a water/ethanol (80/20 by volume) mixture. The precipitated thermoplastic polyurethanes were washed with ethanol and dried at room temperature. The TPUs were then mechanically ground at ambient temperature, washed again, and dried in a vacuum oven at 120 °C. The TPU powders were then compression moulded into solid plaques at elevated temperature (160−200 °C depending on the hard segment concentration). A series of samples with a concentration of hard segment going from 50 to 100 wt % were synthesized. For the synthesis of the 100% hard segment sample, pure Suprasec MPR was used instead of the prepolymer. Finally, a sample of 6.3 wt % hard segment concentration, corresponding to a 1:1 molar ratio between polyol and MDI, was prepared by bulk polymerization at 80 °C in the presence of 0.25% DABCO catalyst. No chain extender was used for the synthesis of this last sample. The TPU samples were stored in a desiccator under a dried atmosphere until use. Samples are designated according to the following nomenclature: PU-*XX*%HS, where *XX* indicates the hard segment concentration by weight of the sample.

Gel Permeation Chromatography. GPC was used to determine the molecular weights of the TPUs (see Table 1). A dilute solution (0.2% of polymer) was prepared in tetrahydrofuran (THF) and stirred overnight. The solutions were filtered through a 0.2 μm polyamide filter. The measurements were performed by Rapra Technology Ltd. at 30 °C using a polystyrene calibration and therefore the molecular weights are given in polystyrene equivalent.

Thermogravimetric Analysis. TGA measurements were performed by ULIRS Thermal Methods Service using a Shimadzu thermogravimetric analyzer (TG-50). The experiments were carried out under nitrogen using alumina crucibles. Samples were heated from room temperature to 800 °C with a scanning rate of 20 °C/min.

Wide-Angle X-ray Scattering. WAXS experiments were carried out on a Guinier X-ray camera. A fixed copper target was used and run under operating conditions of 30 mA and 40 kV. A bent quartz monochromator was used to select the Cu Kα_1 radiation (0.15405 nm). The chamber containing the film, sample holder, and guard slits was evacuated to reduce parasitic scattering from air. After the experiments the X-ray films were scanned and the scattering profile extracted.

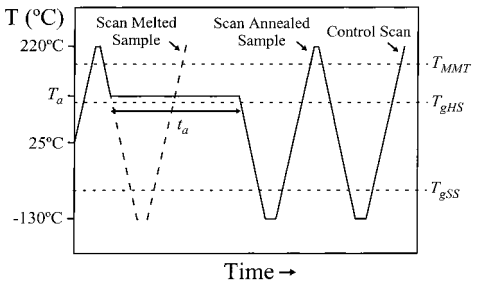

Figure 1. Thermal protocol used for the DSC experiments. The melt-quenched samples (dotted line) are melted 2 min at 220 °C, 40 °C above the highest melting endotherm T_{MMT}, and then quenched at low temperature −130 °C, below the soft segment glass transition T_{gSS}. The DSC thermograph of the so-called melt-quenched samples are recorded during the following heating scan. The annealed samples (solid line) are melted 2 min at 220 °C and then cooled directly to the annealing temperature T_a and kept at this temperature for an annealing time t_a. After annealing the samples are quenched at low temperature, −130 °C. The DSC thermograph of the so-called annealed samples are recorded during the following heating scan. After melting again for 2 min at 220 °C, the annealed samples are quenched at low temperature, −130 °C, and the so-called control thermographs are recorded during the following heating scan.

Differential Scanning Calorimetry. DSC measurements were performed using a Perking-Elmer Pyris 1 apparatus with a liquid nitrogen cooler under nitrogen atmosphere. Zinc and indium were used for a two-point calibration. Indium was used to calibrate the heat capacity. 7 to 11 mg of material was cut out from the moulded plates and introduced in an aluminum pan that was not hermetically sealed. The weight of the aluminum pan was measured before and after DSC experiments to ensure that there was no loss of material resulting from degradation. Figure 1 summarizes the DSC protocol used in this study for the so-called melt-quenched and annealed samples. The samples were initially melted at 220 °C and kept at this temperature for 2 min to clear all previous thermal history. All the thermal cycles were made directly in the DSC apparatus except for the very long annealing time experiments ($t_a > 8$ h) for which an oven preset at the annealing temperature was used. No significant difference was observed in the thermographs obtained for samples annealed the same time at the same temperature in the oven or directly in the DSC apparatus. If no other indications are given, it as to be assumed that the DSC cycles were carried out at 20 °C/min. From all thermographs presented in this study, a baseline, obtained by running an empty pan in the same conditions as the sample, was subtracted and, for comparison purposes, all the thermographs were normalized by the weight of the sample. The analysis of the thermographs was carried out with the Perkin-Elmer Pyris Manager 2.04 software furnished with the instrument. For the endotherms the transition temperature was taken at the maximum of the peak and for the glass transition at the midpoint.

Results and Discussion

Thermal Stability. TGA and GPC were used in order to check the influence, on the samples, of the different thermal treatments used in our study. TGA experiments were performed in the same conditions as DSC experiments, i.e., at 20 °C/min and under nitrogen atmosphere. Figure 2 shows the weight loss as a function of the temperature for three samples: PU-50%HS, PU-75%HS, and PU-100%HS. Significant weight loss starts to be observed for temperatures around ∼300 °C, which are well above the melting temperature used in this study (220 °C). After 1 h at 220 °C the measured weight loss for these samples is less than 3%. However, chain scission events and possible recombination (e.g.,

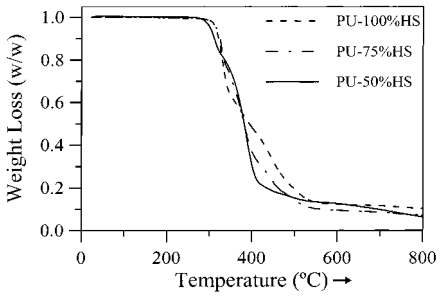

Figure 2. TGA thermographs obtained at 20 °C/min for three samples: PU-50%HS, PU-75%HS, and PU-100%HS.

Table 2. Average Molecular Weight and Polydispersities in Polystyrene Equivalent of the PU-65%HS and PU-85%HS Samples after Different Thermal Treatments

thermal treatment	PU-65%HS			PU-85%HS		
	M_w	M_n	M_w/M_n	M_w	M_n	M_w/M_n
powder	30600	10300	3.0	44600	12900	3.5
moulded plates	38200	12500	3.1	33400	11300	3.0
10 min at 220 °C	38500	11800	3.3	30900	10600	2.9
70 h at 120 °C	38700	11700	3.3	32100	11300	3.0
70 h at 160 °C	131000	14500	9.1	68100	12300	5.7

via cleavage of urethane linkages) are not detected by TGA. Usually, this kind of side reaction induces a change in the molecular weight and/or molecular weight distribution of the samples.[8−10] In Table 2 are presented the molecular weight and molecular weight distribution obtained for PU-65%HS and PU-85%HS after different thermal treatments. Annealing the samples at 160 °C for very long times (70 h) induces a substantial increase in the molecular weights and molecular weight distribution indicating the possible occurrence of a branching reaction. The other thermal treatments, short times at 220 °C and long times at 120 °C, do not affect in a significant way the molecular weights. In this study a sample that went through the complete DSC cycle described in Figure 1 will have spent less than 6 min at 220 °C, and 120 °C is the only annealing temperature used for the purpose of this work. Finally, a control scan is made by DSC (see Figure 1) for all the samples after the annealing experiments to ensure that no difference is observed in the thermograph obtained for the melt-quenched samples before and after the annealing experiments. Having taken these precautions, it seems reasonable to assume for the rest of the discussion that there is no significant degradation occurring in our samples.

Melt-Quenched Samples. In order to study annealing-induced thermodynamic behavior of block-copolymers, it is necessary to first establish a reference state which will be used as a starting point for the annealing experiments and will allow us to check their reproducibility. This is particularly important for linear segmented polyurethanes, which are very sensitive to thermal history. In order to erase all memory of previous thermal histories, the reference state usually used is the melt-quenched state. The samples have to be melted at high temperature in order to disrupt all preexisting structure. In our case this is achieved by melting the samples at 220 °C (40 °C above the highest melting endotherm). In Figure 3 are presented the thermographs obtained after melting the samples 2 min at 220 °C. The heating and the cooling scans were made at 20 °C/min. Using a higher cooling rate or quenching the samples directly in liquid nitrogen after melting does not change significantly the thermographs obtained

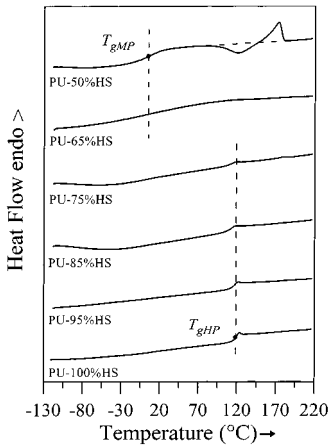

Figure 3. DSC thermographs obtained at 20 °C/min for the melt-quenched TPU samples (for thermal protocol, see Figure 1).

immediately after the quench. The same thermographs were obtained during the control scans made after the annealing experiments (see Figure 1) showing the validity of the melting procedure used in erasing the thermal history of the samples. The validity of this melting procedure was also checked by using the powder samples obtained directly after the synthesis prior to the moulding (i.e., with a different thermal history). Again, the same thermographs as those presented in Figure 3 were obtained after melting the powder samples 2 min at 220 °C.

For the pure hard segment sample (PU-100%HS) a glass transition is detected (see Figure 3) at $T_{gHS} = 119 \pm 2$ °C with an associate heat capacity change of $\Delta C_{pHS} = 0.37 \pm 0.03$ J/(g °C). These values are of the same order of magnitude as those obtained by Cuvé et al. for a series of pure hard segment samples based on MDI diisocyanate.[11] The glass transition of the pure soft segment (PPO-EO) was measured at $T_{gSS} = -73 \pm 2$ °C with an associated heat capacity change of $\Delta C_{pSS} = 0.65 \pm 0.03$ J/(g °C).

There are several equations in the literature that aim to describe the relation between the glass transitions of the pure components and the glass transition of the corresponding homogeneous mixed phase in polymers.[12] The most general form of thermodynamic origin is the Couchman equation[13−15] which is usually approximated for block copolymers such as TPUs by

$$\ln T_{gMS} = \frac{W_{SS}\Delta C_{pSS} \ln T_{gSS} + W_{HS}\Delta C_{pHS} \ln T_{gHS}}{W_{SS}\Delta C_{pSS} + W_{HS}\Delta C_{pHS}} \quad (1)$$

where W_{SS} and W_{HS} are the weight fractions of the soft and the hard segments, respectively. On the other hand, the most general form from empirical origin is the generalized Fox equation:[16]

$$\frac{W_{SS} + kW_{HS}}{T_{gMP}} = \frac{W_{SS}}{T_{gSS}} + \frac{kW_{HS}}{T_{gHS}} \quad (2)$$

where k is the Wood constant which was taken as unity in the original treatment by Fox.[17] Leung and Koberstein[18] extrapolated from their work on a MDI/BDO-based segmented polyurethane a value of ~1.18 for this constant. More recently, Chen et al.[19] were able to fit the glass transitions obtained from melt-quenched sample of another MDI/BDO-based segmented polyure-

thane using a linear weighted combination of the pure constituent values:

$$T_{gMP} = W_{SS}T_{gSS} + W_{HS}T_{gHS} \quad (3)$$

Finally, for the relation between the heat capacity changes of the mixed sample and of the pure components a generally adopted relation is

$$\Delta C_{pMP} = W_{SS}\Delta C_{pSS} + W_{HS}\Delta C_{pHS} \quad (4)$$

In the literature all these equations are usually used to calculate an unknown term which can be a glass transition, a composition, or a heat capacity change. However, it has to be emphasized that the validity of these equations seems to be strongly dependent on the system studied. Indeed, Leung et al.[18] using a polyurethane based on MDI/BDO as hard segment with PPO-EO as soft segment could fit their data for the melt-quenched samples using eqs 2 and 4. By extrapolating to a pure hard segment sample using eq 4, they obtained for the hard segment heat capacity change $\Delta C_{pHS} \sim 0.0$ J/(g °C). On the other hand, more recently, Chen et al.[19] using a polyurethane based on the same hard segment MDI/BDO but with a different soft segment (epoxidized hyroxyl-terminated *cis*-polybutadiene−EHTPB) could fit their results for the melt-quenched samples using eqs 3 and 4 but in this case by extrapolation of eq 4 to pure hard segment sample they obtained $\Delta C_{pHS} \approx 0.38$ J/(g °C) which is in good agreement with the value measured for the PU-100%HS sample. The discrepancy in the values of ΔC_{pHS} obtained by these authors clearly shows that these equations have to be used with caution especially when they are used to evaluate unknown parameters.

For the PU-50%HS sample, after melting and quenching a broad glass transition characteristic of a phase mixed system is detected at $T_{gMP} = 1 \pm 4$ °C with an associated heat capacity change of $\Delta C_{pMP} = 0.60 \pm 0.03$ J/(g °C) (see Figure 3). It is interesting to note that for this sample, for which a homogeneous mixed phase is obtained after melting and quenching, all the parameters of eqs 1, 2, 3, and 4 are known and we can therefore check the validity of these equations for our system. The calculated values obtained for the glass transition and the heat capacity change of the mixed phase are as follows:

equation 1 (Couchman): $T_{gMP} = -18$ °C

equation 2 (Fox): $T_{gMP} = -1$ °C for $k = 1.18$

$T_{gMP} = -8$ °C for $k = 1$

equation 3 (linear combination):

$T_{gMP} = 23$ °C

equation 4: $\Delta C_{pMP} = 0.51$ J/(g °C)

A reasonable agreement is obtained through eq 4 between the measured and the calculated values of ΔC_{pMP}. The best agreement between the measured and the calculated value for T_{gMP} is obtained using the generalized Fox equation. Therefore, we will use in our case the generalized Fox equation with $k = 1.18$ to give an estimation of the purity of the different phases present in our samples.

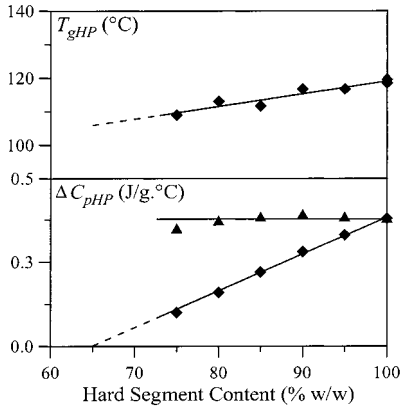

Figure 4. Temperatures T_{gHP} (◆, upper graph), heat capacity changes ΔC_{pHP} (◆, lower graph), and corrected heat capacity change ΔC_{pHPCor} obtained through eq 5 (▲, lower graph) of the hard phase glass transition detected for the melt-quenched samples (see Figure 3) versus the hard segment content C_{HS}.

For samples with concentrations in hard segment of 75% or higher, a glass transition (T_{gHP}) at a temperature close to T_{gHS} is detected after melting and quenching the samples (see Figure 3), indicating the presence of an almost "pure" hard segment phase. In Figure 4 are presented the temperature, T_{gHP}, and the associated heat capacity change, ΔC_{pHP}, of the hard segment phase glass transition as a function of hard segment concentration. A relatively small diminution of T_{gHP} with decreasing hard segment concentration is observed. This diminution could indicate that some soft segments are present in this hard segment phase. If we use eq 2 to estimate the weight fraction of soft segment present in this hard segment phase, we obtain 3% (w/w) for the PU-75%HS sample. Another factor, which is likely to be also at the origin of a decrease in T_{gHP}, is the diminution of the average hard block length[20] with increasing soft segment concentration (see Table 1). For block copolymers the molecular weight of the different segments is a function of the initial concentration of the different elements and can be affected by the synthetic route used to polymerize the block copolymer.[21−23]

The heat capacity change ΔC_{pHP} associated with the hard segment phase glass transition decreases linearly with decreasing hard segment concentration. By extrapolation of the linear regression, $\Delta C_{pHP} = 0$ is obtained for a concentration of 65% hard segment (see Figure 4). Indeed, no T_{gHP} is observed for PU-65%HS sample (see Figure 3). If we assume that this hard segment phase is formed only by hard segments and if we correct the measured values of ΔC_{pHP} for the hard segment concentration of the samples, we do not obtain for the corrected heat capacity change a value corresponding to the pure hard segment sample PU-100%HS. This implies that a significant part of the hard segments are not residing in this hard segment phase but are incorporated with the soft segments in a mixed phase. This is confirmed by the fact that no typical low-temperature glass transition corresponding to a soft segment phase (T_{gSP}) is observed (see Figure 3). When the samples are annealed, as will be discussed later, T_{gSP} can be clearly detected for the PU-65%HS sample.

Let us assume that this mixed phase has a weight ratio between hard and soft segment of $C_{MP} = 65/35 = 1.8$ (corresponding to 65% hard segment concentration). If we correct the measured heat capacity from the hard segment concentration and from the hard segment incorporated in the mixed phase through the relation

$$\Delta C_{\mathrm{pHPCor}} = \Delta C_{\mathrm{pHP}}\left[\frac{100}{C - C_{\mathrm{MP}}(100 - C)}\right] \qquad (5)$$

where C (wt %) is the hard segment concentration of the sample and $\Delta C_{\mathrm{pHPCor}}$ the corrected heat capacity of the hard segment phase, then $\Delta C_{\mathrm{pHPCor}}$ agrees within the limit of experimental errors with the value obtained for the pure hard segment sample (see Figure 4). This observation suggests that for a hard segment concentration higher than 65% the melt-quenched samples are not in a homogeneous mixed phase. Part of the hard segments is incorporated with the soft segments in a mixed phase with a stoichiometry of ∼1.8 (65% hard segment) and the rest forms an almost pure hard segment phase. This value of 1.8 could be seen as the amount in grams of hard block which can be "dissolved" per gram of soft block.

As already mentioned, the PU-65%HS sample did not present any T_{gHP} after it had been melted and quenched, but on the other hand a clear T_{gMP}, like the one observed for the PU-50%HS sample, could not be observed. A careful examination of the thermograph in Figure 3 reveals the presence of what could be a very broad glass transition stretching over 50−70 °C. This kind of broadening has already been reported for TPUs[24] and semicrystalline polymers. In this latter case, the broadening of the glass transition is usually ascribed to a large variation of the segmental mobility of the amorphous phase due to the mobility restriction imposed by the crystalline regions.[25] In the case of TPUs this restriction could be due to the hard phase regions whose mobility is much lower than the mixed phase regions. As a result of this mobility restriction the mixed phase glass transition is not observed for the sample with higher hard segment content. Solid-state NMR experiments on these materials should allow us to clarify this point.

Finally, for the PU-50%HS sample, when melted and quenched, after the mixed phase glass transition, T_{gMP}, an exotherm followed by an endotherm are observed (see Figure 3). This kind of behavior has already been observed for other polyurethanes.[6,3] The enthalpies of these two transitions are very close, suggesting that they have the same physical origin. In Figure 5 are presented the thermographs obtained for this sample using a particular DSC sequence. The thermograph at the top of Figure 5 corresponds to the melt-quenched sample. After melting and quenching, the sample is heated to 125 °C, just over the exotherm peak (thermograph 1, Figure 5). The glass transition T_{gMP}, indicating that the sample is phase mixed, is detected. Then the sample is cooled to −130 °C and heated again (thermograph 2, Figure 5). In this thermograph, T_{gMP} is no longer observed and, instead, a glass transition at low temperature (close to the glass transition measured for the pure soft segments) $T_{\mathrm{gSP}} = -64 \pm 3$ °C corresponding to an almost pure soft segment phase is detected, indicating that the sample is now phase separated. The exothermic transition is no longer observed but the endothermic peak is still present. If after 2 min at 220 °C we cool the sample one last time and heat it again (thermograph 3, Figure 5), the T_{gSP} is no longer observed but the T_{gMP} indicating a phase mixed system and the exotherm and endotherm are present again. This behavior suggests that the exotherm (T_{MST}) and the endotherms (T_{MMT}) observed after melting and quenching the PU-50%HS sample are associated with the microphase demixing and mixing of the sample. It should also be noted that no diffraction peaks are observed after annealing the sample for a few seconds at 120 °C, giving no sign of the presence of a crystalline or a large scale ordered structure. As will be discussed later, weak diffraction peaks can be observed after annealing the samples for long times at 120 °C.

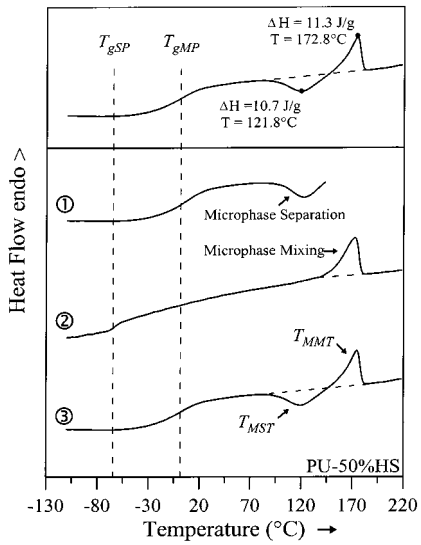

Figure 5. Upper graph: DSC thermograph of the melt-quenched PU-50%HS sample. Lower graph: DSC thermographs of the chained experiment 1 → 2 → 3 for the PU-50%HS sample (for details see text).

Isothermal Annealing at 120 °C. In this section we will present the results of the isothermal annealing experiments obtained using the DSC protocol described in Figure 1 for three samples: PU-50%HS, PU-65%HS, and PU-85%HS. For the purpose of this article we will present only the results obtained using 120 °C as annealing temperature. The effect of the annealing temperature, and in particular sub-T_{gHS} annealing temperatures, on the phase behavior of this set of samples will be presented in a forthcoming article. In Figures 6, 8, and 11, the thermographs obtained for these samples after annealing for different annealing times (t_a) at 120 °C are presented, and in Figures 7, 9, and 12 the temperatures, enthalpies, and heat capacity changes of the different thermal events detected are plotted as a function of log(t_a).

PU-50%HS. As seen in the previous section after melting and quenching, this sample is phase mixed and presents a broad glass transition around 1 °C. When heated at 120 °C, an exothermic transition, which could be related to the phase demixing of the sample, is detected. In the following DSC scan a low-temperature glass transition ($T_{\mathrm{gSP}} = -64 \pm 3$ °C) corresponding to a soft segment phase is detected (see Figure 5). When the samples are annealed at 120 °C, T_{gSP} is always detected at around the same temperature: −64 °C (see Figure 6). The difference between T_{gSP} and the glass transition temperature measured for the pure soft segment sample can partly be accounted for by a mobility restriction effect due to the anchoring of the soft segments to the hard blocks.[19] Indeed the glass transition of the PU-6.3%HB sample, corresponding to all soft segments being encapsulated with one MDI unit, is measured at −67 ± 3 °C. The heat capacity change is also slightly affected by the presence of MDI units (0.62 ± 0.03 J/(g °C) is obtained for the PU-6.3%HS sample). Another

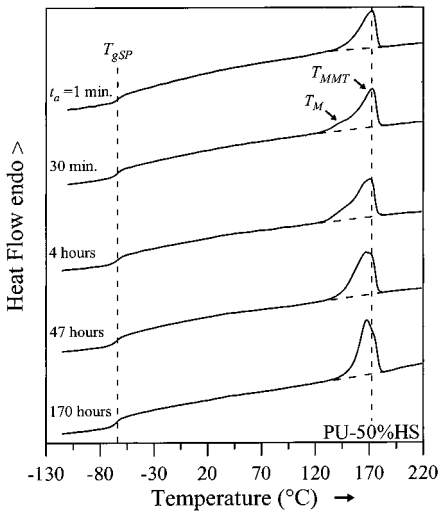

Figure 6. DSC thermographs obtained at 20 °C/min for the PU-50%HS sample annealed for different annealing times t_a at 120 °C (for thermal protocol see Figure 1).

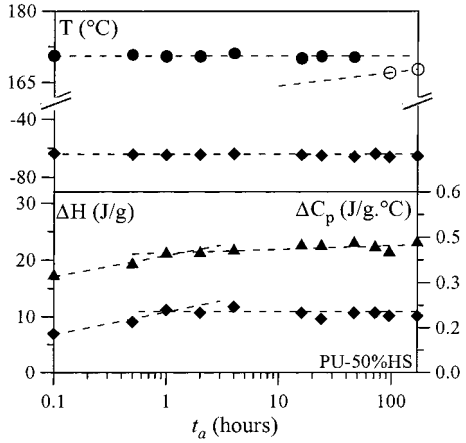

Figure 7. Temperatures, enthalpies, and heat capacity changes of the transitions observed via DSC for the PU-50%HS sample annealed for different annealing times t_a at 120 °C (see Figure 6) versus the logarithm of t_a. Upper graph: temperatures of the endothermic transitions T_M (○) and T_{MMT} (●) and of the soft phase glass transition T_{gSP} (◆). Lower graph: total enthalpy of the endothermic transitions ΔH_{Tot} (▲) and heat capacity change of the soft phase glass transition ΔC_{pSP} (◆).

factor, which could also be contributing to this difference, is the presence of some hard segments in this soft segment phase. If we estimate through eq 2 the weight fraction of hard segment present in this soft phase taking −67 °C for T_{gSS}, we obtain ∼3% for W_{HS}, which suggests that this soft segment phase is almost "pure". The fact that T_{gSP} is constant indicates that the overall "purity" of this soft phase is not affected by the annealing time. On the other hand, as can be observed in Figure 7, the heat capacity change, ΔC_{pSP}, associated with T_{gSP} is increasing with increasing t_a for the first hour of annealing and then becomes constant for longer t_a. The increase in ΔC_{pSP} indicates that more and more soft segments are taking part in this soft segment phase, suggesting an increase in the degree of phase separation during the first hour of annealing. Once the level of phase separation is maximum for these annealing conditions, ΔC_{pSP} becomes constant.

In addition to the endothermic peak assigned previously to the microphase mixing transition (T_{MMT}), a second endothermic peak is detected (T_M) at lower temperature when the sample is annealed. The temperature of T_M seems to increase with increasing t_a, as can be seen from the long annealing time experiments when T_M becomes predominant (see Figure 6). On the other hand, T_{MMT} seems not to be affected significantly. As these two endotherms are too close to be resolved for this sample, it is not possible to evaluate their individual enthalpies with reasonable certainty. However, from Figure 7 it can be seen that the total enthalpy ΔH_{Tot} of these two transitions increases rapidly up to 1 h of annealing and then more slowly for longer t_a, suggesting some correlation between the variation of the heat capacity change associated with the soft segment phase glass transition and the enthalpies of the melting endotherms.

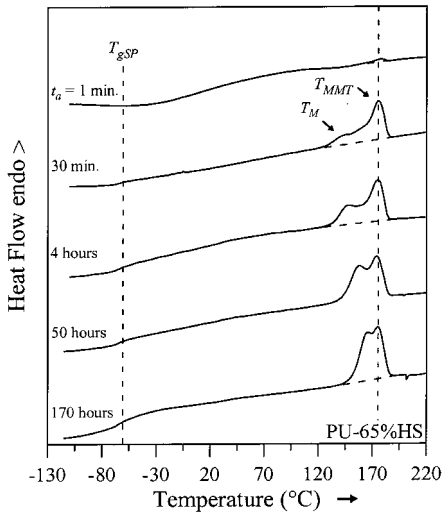

Figure 8. DSC thermographs obtained at 20 °C/min for the PU-65%HS sample annealed for different annealing times t_a at 120 °C (for thermal protocol see Figure 1).

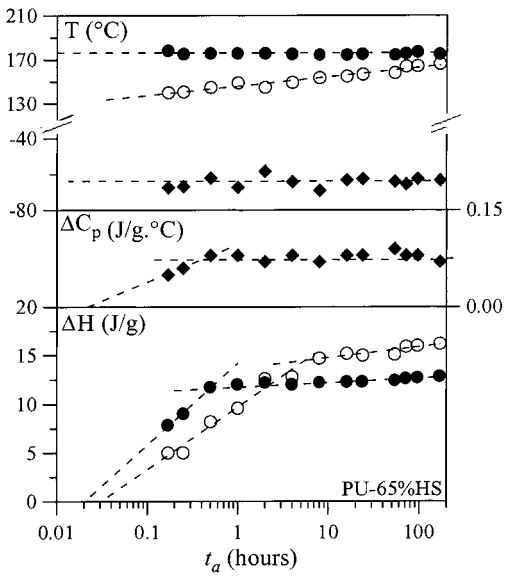

Figure 9. Temperatures, enthalpies, and heat capacity changes of the transitions observed via DSC for the PU-65%HS sample annealed for different annealing times t_a at 120 °C (see Figure 8) versus the logarithm of t_a. Upper graph: temperatures of the endothermic transitions T_M (○) and T_{MMT} (●) and of the soft phase glass transition T_{gSP} (◆). Middle graph: heat capacity changes of the soft phase glass transition ΔC_{pSP} (◆). Lower graph: enthalpies of the endothermic transitions ΔH_M (○) and ΔH_{MMT} (●).

PU-65%HS. As seen earlier, after melting and quenching no low-temperature glass transition is observed for

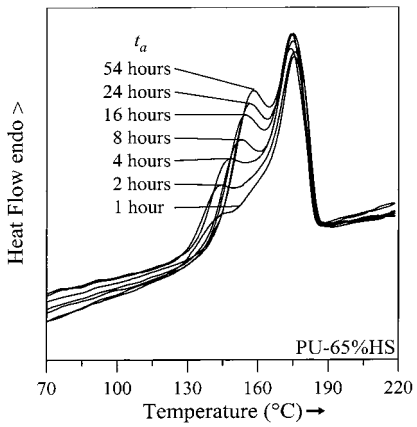

Figure 10. Superposed DSC thermographs obtained at 20 °C/min for the PU-65%HS sample annealed for different annealing times t_a at 120 °C (for thermal protocol see Figure 1).

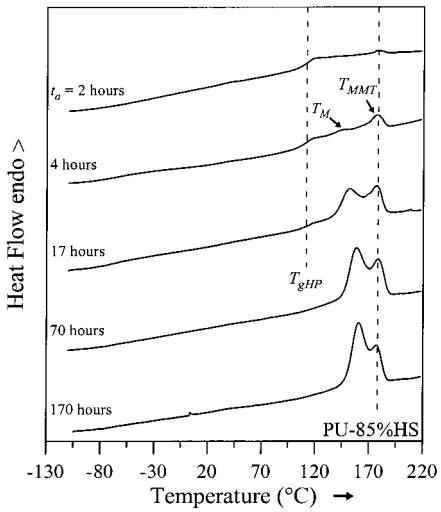

Figure 11. DSC Thermographs obtained at 20 °C/min for the PU-85%HS sample annealed for different annealing times t_a at 120 °C (for thermal protocol see Figure 1).

this sample. From Figure 8 it can be seen that with increasing t_a a low-temperature glass transition (T_{gSP}) appears at about the same temperature, −64 °C, as for the PU-50%HS sample, suggesting that during annealing this sample undergoes phase separation. As for the previous sample, T_{gSP} is not affected by t_a while the heat capacity change ΔC_{pSP} increases up to 30 min of annealing and then becomes constant. Here again the increase of ΔC_{pSP} suggests an increase in the degree of phase separation of this sample during the first 30 min of annealing.

From Figure 8 we can observe that for this sample with increasing t_a two endothermic transitions are growing at high temperature: T_M and T_{MMT}. The low-melting endotherm temperature T_M increases with increasing t_a while the high-melting endotherm temperature T_{MMT} is constant. The difference between the thermodynamic behavior of these two endotherms can clearly be seen from Figure 10 where the thermographs obtained for t_a ranging from 1 to 54 h have been superposed. In this case the two endotherms being more widely spaced it was possible to estimate the enthalpies (ΔH_M and ΔH_{MMT}) associated with each of them. As can be seen from Figure 9, ΔH_{MMT} is varying in a similar way to ΔC_{pSP} increasing up to 30 min annealing and then becoming constant, while two regimes are observed

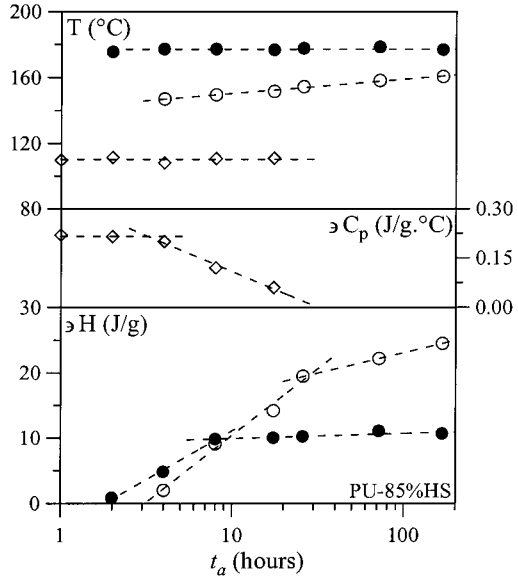

Figure 12. Temperatures, enthalpies, and heat capacity changes of the transitions observed via DSC for the PU-85%HS sample annealed for different annealing times t_a at 120 °C (see Figure 11) versus the logarithm of t_a. Upper graph: temperatures of the endothermic transitions T_M (○) and T_{MMT} (●) and of the soft phase glass transition T_{gSP} (◆). Middle graph: heat capacity changes of the soft phase glass transition ΔC_{pSP} (◆). Lower graph: enthalpies of the endothermic transitions ΔH_M (○) and ΔH_{MMT} (●).

in the variation of ΔH_M increasing "fast" for t_a < 6 h and "slow" for t_a > 6 h.

The similarity in the variations of ΔC_{pSP} and ΔH_{MMT} confirms the correlation between the glass transition of the soft segment phase and the high-temperature melting endotherm T_{MMT}. It supports the assignment, suggested previously, of this endotherm to the microphase mixing transition of the sample, ΔH_{MMT} corresponding then to the mixing enthalpy. It is then expected that the mixing enthalpy increases with increasing degree of phase separation, in other words with increasing ΔC_{pSP}, and then becomes constant when ΔC_{pSP} becomes constant. The difference in the thermodynamic behavior of these two melting endotherms suggests that they have different physical origins. It is well-known that 4,4′-MDI-based hard segments are able to establish ordered structures under certain conditions[26,27] and annealing at temperatures higher than the glass transition of the hard segments favors this ordering. The appearance of weak diffraction peaks with increasing t_a confirms the growth in these samples of an ordered structure. This could mean that the lower temperature melting endotherm T_M corresponds to the melting of this ordered structure. The increase of T_M and ΔH_M with increasing t_a is consistent with this interpretation as we will see for the next sample.

PU-85%HS. For this sample, as said previously, after melting and quenching a high-temperature glass transition, T_{gHP}, is detected corresponding to an almost pure hard segments phase (see Figure 3). T_{gHP} is constant with increasing t_a while the heat capacity change (ΔC_{pHP}) associated with this glass transition is constant up to ∼3 h annealing and then decreases and becomes zero for ∼24 h annealing (see Figure 12). The decrease of ΔC_{pHP} suggests the ordering/crystallization of the hard segments. The glass transition being characteristic of the hard segments in the amorphous state, once this ordered structure is established, it will not present a

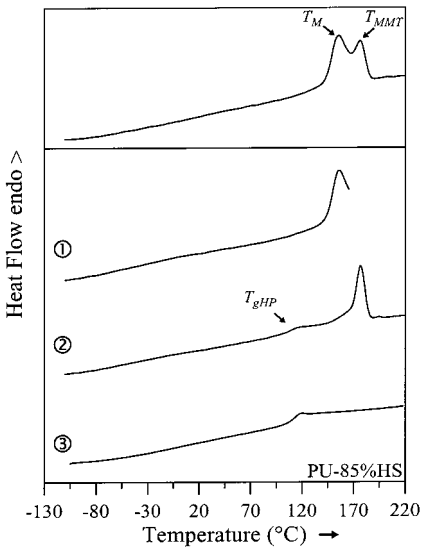

Figure 13. Upper graph: DSC thermograph of the PU-85%HS sample annealed 72 h at 120 °C. Lower graph: DSC thermographs of the chained experiment 1 → 2 → 3 for the PU-85%HS sample (for details see text).

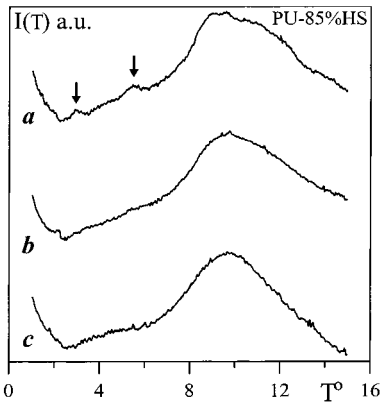

Figure 14. Wide-angle X-ray diffracted intensity $I(\theta)$ versus the scattering angle θ for the PU-85%HS sample: (a) annealed 72 h at 120 °C, (b) annealed few seconds at 167 °C, and (c) melted 2 min at 220 °C.

glass transition any more but a melting endotherm corresponding to the disruption of the ordered structure. This is confirmed by the appearance of diffraction peaks on the wide-angle scattering pattern with increasing t_a (see Figure 14a). It has to be noted that the diffraction peaks, as usual for 4,4′-MDI/BDO-based TPUs,[5,4] are few and very weak, suggesting that only a very weakly ordered structure is present in this hard segment phase. Nevertheless, the presence of these diffraction peaks indicates that some kind of order is appearing in the sample after long annealing times.

For this sample also two endothermic transitions appear with increasing t_a. The overall behavior of the enthalpies and the temperatures of these two endotherms is similar to that observed for the PU-65%HB sample but the time scales involved are longer. If the same assignments as for the previous samples are made then for this sample the phase separation is maximum after 8 h (see Figure 12). This difference in time scales could be related to the difference in viscosity of these two samples. Indeed it is expected as the concentration in hard segments is increased that the viscosity of the sample is increased and the dynamics slowed. For this sample also two regimes are found for the increase of ΔH_M, a "fast" regime for $t_a < 24$ h and a "slow" regime for $t_a > 24$ h. It should also be noted that T_{MMT} is first detected after 2 h annealing while T_M takes 3 h annealing to appear, suggesting that phase separation is the first process to start rather than the ordering of the hard phase.

As can be seen from Figure 12 the variations of ΔC_{pHP} and ΔH_M are correlated. In particular, when ΔC_{pHP} decreases ΔH_M increases, suggesting that T_M corresponds to the melting of the ordered structure that appears with annealing in the hard segment phase. To confirm this assignment, the set of DSC experiments illustrated in Figure 13 was made. On the top graph is presented the DSC thermograph obtained for a sample annealed 72 h at 120 °C. Two melting endotherms, T_M and T_{MMT}, are detected by DSC and several diffraction peaks are observed via WAXS (see Figure 14a). A first DSC scan is made by heating the sample to 167 °C, just over the T_M endotherm (thermograph 1, Figure 13). Then the sample is quenched at low temperature and the diffraction pattern recorded again. As can be seen in Figure 14b, the diffraction peaks have almost completely disappeared, suggesting the disruption of the ordered structure. This is confirmed by the following DSC scan showing again the presence of a T_{gHP} indicating that the hard segments are again in an amorphous state (thermograph 2, Figure 13). It should be noted that the endotherm T_M has almost completely disappeared while the endotherm T_{MMT} is still present. Finally, if the sample is melted 2 min at 220 °C and cooled, the same thermograph as for the melt-quenched sample is obtained (thermograph 3, Figure 13) and the diffraction peaks have completely disappeared (see Figure 14c). This experiment confirms the relationship between the diffraction peaks observed and endotherm T_M suggesting that this transition corresponds to the melting of the ordered structure appearing in the hard segment phase during annealing.

As already mentioned before, the variations of T_M and ΔH_M are consistent with the assignment of this transition to the melting of the ordered structure. Indeed, for crystalline or semicrystalline polymers when isothermally annealed an increase in the melting enthalpy and temperature is usually observed due to an increase in crystallinity and crystal perfection.[25] It is interesting to observe that the change in the slope of ΔH_M is observed when ΔC_{pHP} becomes zero. This might suggest that when the secondary interactions between hard segments become strong enough to restrict their mobility the ordering process is slowed. It is well-known that hydrogen bonding between hard segments in polyurethane materials plays an important role in the dynamics of crystallization and phase separation. Infrared investigations are under way to try to understand the role of hydrogen bonding in the thermodynamic behavior of this set of samples.

Isochronal Annealing at 120 °C. In Figure 15 are presented the thermographs obtained after annealing all the samples 72 h at 120 °C and Figure 16 shows, as a function C_{HS}, the hard segment concentration, the enthalpies, and temperatures of the melting endotherms T_M and T_{MMT}.

As noted previously, segmental mobility plays an important role in the dynamics of TPUs. In particular, the time for the phase separation to reach its maximum depends on the hard segment concentration.[28] It turns out in this case, annealing at 120 °C, that after 72 h

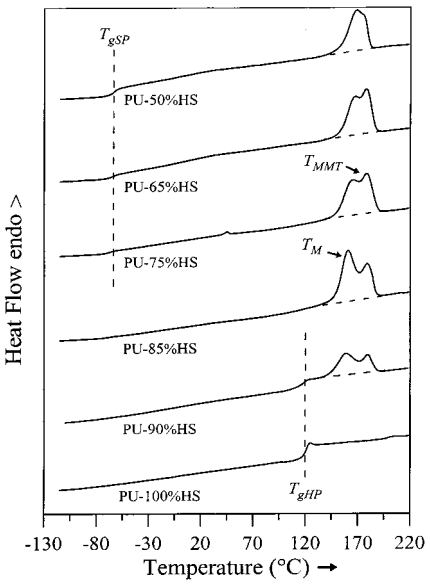

Figure 15. DSC thermographs obtained at 20 °C/min for the TPU samples annealed 72 h at 120 °C (for thermal protocol see Figure 1).

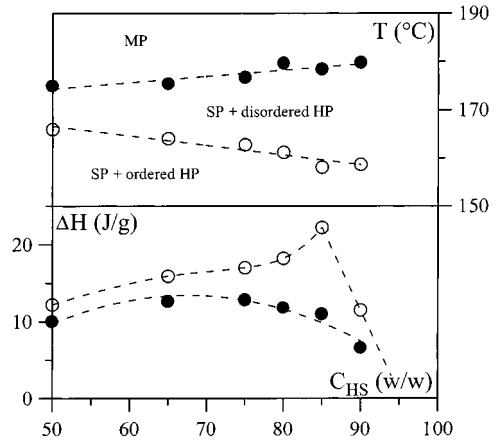

Figure 16. Temperatures and enthalpies of the transitions observed via DSC for the TPU samples annealed for 72 h at 120 °C (see Figure 15) versus the hard segment content C_{HS}. Upper graph: temperatures of the endothermic transitions T_M (○) and T_{MMT} (●) and the different phase domains: SP, soft phase; HP, hard phase; and MP, mixed phase. Lower graph: enthalpies of the endothermic transitions ΔH_M (○) and ΔH_{MMT} (●).

annealing ΔH_{MMT} has already reached its maximum value for all the samples. As can be seen from Figure 16, T_{MMT} is increasing slightly with increasing C_{HS}. On the other hand, ΔH_{MMT} seems to be going through a maximum for a concentration of ~65% hard segments. This again supports the assignment made before for this transition that it is caused by the microphase mixing of the sample. Indeed it is expected for a mixing enthalpy to be related to the hard/soft segment ratio, being maximum for the stoichiometric concentration of the mixed phase (~65%) and being zero for the pure soft and hard segment samples provided that the degree of phase separation is the same for all the samples.

The comparison between the values obtained for T_M and ΔH_M is more ambiguous due to the fact that, as seen above, the ordering/crystallization time of the hard segments is also dependent on the hard segment concentration but in this case even after long annealing times the melting enthalpy and temperature continue to increase. For the same annealing time, depending on the hard segment concentration, the samples are in a different stage of the crystallization process as confirmed by the PU-90%HS sample. In this case we can observe that even after 72 h a significant hard segment phase glass transition, T_{gHP}, can be detected. If we anneal this sample for longer times at 120 °C, we observe a decrease in ΔC_{pHP} and an increase in ΔH_M and T_M, while ΔH_{MMT} is already maximum. Nevertheless, the sharp decrease of ΔH_M for $C_{HS} > 85\%$ underlines the important plasticizing role played by the soft segments in high hard block content TPUs. Introducing in our case 15% of soft segments increases in a significant way the mobility of the system inducing an increase in the ordering rate of the hard segments.

Table 3. ΔC_{pSP}: Soft Phase Glass Transition Heat Capacity Change[a]

samples	ΔC_{pSP} (J/g °C)	$\Delta C_{pSP\ Cor}$ (J/g °C)	$\Delta C_{pSPCor}/\Delta C_{pSS}$
PU-50%HS	0.21 ± 0.02	0.42 ± 0.04	0.68 ± 0.10
PU-65%HS	0.09 ± 0.02	0.26 ± 0.06	0.42 ± 0.12
PU-75%HS	0.025 ± 0.02	0.10 ± 0.08	0.16 ± 0.14

[a] $\Delta C_{pSP\ Cor}$: soft phase glass transition heat capacity change corrected for the samples hard segment content. ΔC_{pSS}: soft segments glass transition heat capacity change. (For details see text.)

For samples with a hard segment concentration lower than 80%, the soft segment phase glass transition, T_{gSP}, can be clearly detected (see Figure 15). In Table 3 are reported the measured values for the heat capacity change, ΔC_{pSP}, associated with this glass transition. In this table are also reported ΔC_{pSPCor}, the heat capacity change per gram of soft segments present in the sample and the ratio $\Delta C_{pSPCor}/\Delta C_{pSS}$ which is usually used for low hard segment content TPUs as a measure of the degree of phase separation.[24] As can be seen from Table 3, ΔC_{pSPCor} decreases with increasing hard segment concentration, indicating that not all the soft segments present in the samples are contributing to this soft segment phase glass transition. One explanation for these "missing" soft segments could be that they are not phase separated and still mixed with some hard segment in a mixed phase. But as we saw previously even for high hard segment concentration, a T_{MMT} endotherm assigned to the phase mixing can be observed, suggesting that even for these samples some degree of phase separation is present even if no T_{gSP} is observed. A more likely explanation could be that some of the soft segments have a restricted mobility due to their vicinity to the hard segment regions and therefore do not present a glass transition. These "missing" soft segments could be part of an interphase with a restricted mobility between the hard and soft domain. In these conditions the determination of the phase separation degree from the soft segment phase glass transition does not seem to be adequate for high hard block content TPUs.

Conclusions

The thermodynamic behavior of a set of high hard block content TPUs has been investigated using mainly DSC. By correlating the behavior of the different observed transitions this work suggests that the two melting endotherms observed at high temperature are related to the melting of an ordered structure appearing in the hard phase (T_M) and to the microphase mixing of the soft and hard segments (T_{MMT}). These results are

in agreement with the work of A. J. Ryan et al.[7] For a similar system using DSC, SAXS, and DMA these authors have observed the presence of an order−disorder transition corresponding to the microphase mixing of the soft and hard segments in the same range of temperature. In the case of their systems, because of the utilization of a mixture of 2,4′- and 4,4′-MDI for the hard segment, no ordering was observed in the hard phase.

These assignments suggest a two-step melting process for our samples: in the first stage melting of the ordered structure present in the hard phase, and in the second stage the microphase mixing of the soft and hard segments (see Figure 16). Annealing experiments at 120 °C also suggest that for high hard block content polyurethane, phase separation is the first process to start followed by the ordering of the hard phase.

Finally, for the melt-quenched samples our results show that for a hard segment content smaller than 65% a homogeneous mixed phase is obtained while for higher hard block content a two-phase system is obtained.

To elucidate further the interpretation of our DSC results a structural investigation has been carried out using mainly small-angle X-ray scattering combined with DSC and transmission electron microscopy. These results will be presented in a forthcoming article.

Acknowledgment. The authors gratefully acknowledge ICI plc for their financial support from their strategic research fund.

References and Notes

(1) *Polyurethanes Handbook*; Hanser: Munich, Germany, 1994.
(2) Woods, G. *The ICI Polyurethanes Book*; 1990.
(3) Chen, K. C.; Shieh, T. S.; Chui, J. Y. *Macromolecules* **1998**, *31*, 1312.
(4) Frontini, M. F.; Pavan, A. *J. Appl. Polym. Sci.* **1993**, *48*, 2003.
(5) Koberstein, J. T.; Galambos, A. F. *Macromolecules* **1992**, *25*, 5618.
(6) Phillips, R. A.; Cooper, S. L. *J. Polym. Sci., Part B*: *Polym. Phys.* **1996**, 34, 737.
(7) Ryan, A. J.; Macosko, C. W.; Bras, W. *Macromolecules* **1992**, *25*, 6277.
(8) Hu, W.; Koberstein, J. T. *J. Polym. Sci., Part B*: *Polym. Phys.* **1994**, *32*, 437.
(9) Shieh, Y. T.; Chen, H. T.; Liu, K. H.; Twu, Y. K. *J. Polym. Sci., Part A*: *Polym. Chem.* **1999**, *37*, 4126.
(10) Yang, W. P.; Macosko, C. W.; Wellinghoff, S. T. *Polymer* **1986**, *27*, 1235.
(11) Cuvé, L.; Pascault, J. P.; Seytre, G.; Boiteux, G. *Polymer* **1991**, *32*, 343.
(12) Koberstein, J. T.; Leung, L. M. *Macromolecules* **1992**, *25*, 6205.
(13) Couchman, P. R. *Macromolecules* **1978**, *11*, 117.
(14) Couchman, P. R. *Macromolecules* **1980**, *13*, 1272.
(15) Couchman, P. R. *Polym. Eng. Sci.* **1984**, *24*, 135.
(16) Wood, L. A. *J. Polym. Sci.* **1958**, *28*, 319.
(17) Fox, T. G. *Bull. Am. Phys. Soc.* **1956**, *1*, 123.
(18) Leung, L. M.; Koberstein, J. T. *Macromolecules* **1986**, *19*, 706.
(19) Chen, K. C.; Chui, J. Y.; Shieh, T. S. *Macromolecules* **1997**, *30*, 5068.
(20) Xu, M.; MacKnight, W. J.; Chen, C. H. Y.; Thomas, E. L. *Polymer* **1983**, *24*, 1327.
(21) Peebles, L. H. *Macromolecules* **1974**, *7*, 872.
(22) Peebles, L. H. *Macromolecules* **1976**, *9*, 58.
(23) Chen, C. H. Y.; Briber, R. M.; Thomas, E. L.; Xu, M.; MacKnight, W. J. *Polymer* **1983**, *24*, 1333.
(24) Camberlin, Y.; Pascault, J. P. *J. Polym. Sci., Polym. Chem. Ed.* **1983**, *21*, 415.
(25) Nogales, Z.; Denchev, I.; Šics, T. A. *Macromolecules* **2000**, *33*, 9367.
(26) Briber, R. M.; Thomas, E. L. *J. Polym. Sci., Polym. Phys. Ed.* **1985**, *23*, 1915.
(27) Blackwell, J.; Lee, C. D. *J. Polym. Sci., Polym. Phys. Ed.* **1984**, *22*, 759.
(28) Lee, H. S.; Hsu, S. L. *Macromolecules* **1989**, *22*, 1100.

MA0105993